# Porphyrin/sPEEK Membranes with Improved Conductivity and Durability for PEFC Technology

Carbone, Alessandra; Gaeta, Massimiliano; Romeo, Andrea; Portale, Giuseppe; Pedicini, Rolando; Gatto, Irene; Castriciano, Maria Angela

*Published in:*
ACS Applied Energy Materials

*DOI:*
10.1021/acsaem.8b00126



*Publication date:*
2018

ACS APPLIED ENERGY MATERIALS
Cite This: ACS Appl. Energy Mater. 2018, 1, 1664−1673
Article
www.acsaem.org

# Porphyrin/sPEEK Membranes with Improved Conductivity and Durability for PEFC Technology

Alessandra Carbone,[†] Massimiliano Gaeta,[‡] Andrea Romeo,[‡,§] Giuseppe Portale,[∥] Rolando Pedicini,[†] Irene Gatto,[†] and Maria Angela Castriciano*[,‡]

[†]Istituto di Tecnologie Avanzate per l'Energia "Nicola Giordano", via S. Lucia sopra Contesse 5, 98126 Messina, Italy

[‡]Istituto per lo Studio dei Materiali Nanostrutturati, Dipartimento di Scienze Chimiche, University of Messina Viale Ferdinando Stagno D'Alcontres No. 31, Villaggio S. Agata, 98166Messina, Italy

[§]Dipartimento di Scienze Chimiche, University of Messina Viale Ferdinando Stagno D'Alcontres No. 31, Villaggio S. Agata, 98166 Messina, Italy

[∥]Zernike Institute for Advanced Materials, University of Groningen, NL-9747 AG Groningen, The Netherlands

Supporting Information

**ABSTRACT:** Advanced composite membranes have been obtained by incorporation of the *meso*-tetrakis(4-sulfonatophenyl)porphyrin (TPPS) into a sulfonated poly(etheretherketone) (sPEEK). The presence of porphyrins in their monomeric, dimeric, and aggregated forms into the membrane ionic domains have been investigated by static and time-resolved spectroscopic techniques. In particular, we succeeded in modulating the percentage of the different porphyrin species present into the proton-conducting channels acting on the dye load in the range 0.35−5 wt % porphyrin/polymer. The nanostructure of all the composite membranes has been investigated by small-angle X-ray scattering. This latter shows how the presence of TPPS porphyrins into the membrane ionic domains induces a reorganization of polymer chains in a more stable and organized lamellar-like structure with respect to the pristine polymeric matrix. Finally, the composite membranes have been used as proton exchange membrane for fuel cells (PEFCs) technology. The presence of porphyrins improved the performance of the membranes in terms of proton conductivity and stability. In particular, the 0.77 wt % composite membrane has been tested in a PEFC single cell simulating the operative conditions typical for portable applications, highlighting an improved stability compared to that of the sPEEK pristine membranes.

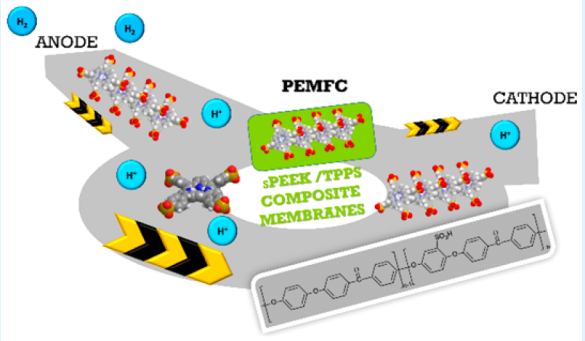


**KEYWORDS:** *composite membranes, sPEEK, porphyrins, aggregation, fuel cells*

## INTRODUCTION

Nowadays, polymer electrolyte fuel cells (PEFCs) are very promising devices for clean energy generation mainly devoted to vehicles as well as to stationary and portable applications.[1] For portable applications, typical fuels are hydrogen or methanol and the oxidant is air coming from the environment. The power demand of portable electronics devices ranges from 1 W for cellular phones to 20−30 W for notebook personal computers.[2] Portable systems of several watts have been developed by Horizon and Myfc companies, demonstrating the benefit of using hydrogen for user-friendly operations.[3] The advantages are safety, longer stability of the components, and higher efficiency (60% for hydrogen vs 25% for methanol). Generally, portable PEFCs have an open cathode configuration, sometimes supported by a small fan, in order to permit a good exposition of the cathode surface to the air, and when hydrogen is used as fuel, it is directly supplied by a tank containing hydride. In this configuration, an auxiliary system, for reagents humidification, is not foreseen and dry hydrogen is supplied, hindering the proton conduction through the membrane and limiting the performance of the device. In addition to a performance increase, the ultimate technical targets established by DoE[4] individuate durability and cost as important requirements for market penetration of portable power fuel cell systems. The proton exchange membrane (PEM) represents one of the most important components influencing performance, durability, and cost of PEFC devices. The presence of specific proton transport channels in the membrane plays a key role for obtaining high performance materials.[5] This goal is usually achieved by introducing specific functional acid groups into polymeric structures.[6−8] Perfluorosulfonic membranes such as Nafion are the most used materials even if they show working limits related to their high production costs as well as low stability at high temperature due to low glass

Received: January 30, 2018
Accepted: March 23, 2018
Published: March 23, 2018






DOI: 10.1021/acsaem.8b00126
ACS Appl. Energy Mater. 2018, 1, 1664−1673

transition of the polymeric matrix.[9] In this framework, sulfonated aromatic hydrocarbon-type polymers can be considered as a good alternative to Nafion. Indeed, due to their rigid aromatic backbone these polymers have shown high thermal stability and mechanical strength together with low production costs.[10−14,8] Currently, sulfonated poly(ether ether ketone) (sPEEK) is used in fuel cells technology as an acidic polymeric matrix showing interesting performance in terms of high proton conductivity and good mechanical properties as well as reduced hydrogen crossover and costs.[11,15] Small-angle X-ray scattering (SAXS) investigation has shown how the nanostructure of these membranes is strictly related to the polymer ion-exchange capacity.[16,5] Structural and chemical physical modifications have been reported as a function of different parameters such as (i) water load[17] and the nature of the counterion,[18,12] (ii) membrane treatment,[19−21] (iii) level of sulfonation,[16] and (iv) presence of strong or weak acid.[7] In order to improve the mechanical properties of the polymeric matrix, in particular at high temperature operative conditions, advanced composite membranes have been obtained by introducing inorganic or organic fillers into the pure polymer, thus achieving stabilization through the occurrence of strong covalent or weak supramolecular interactions.[22] In particular, sPEEK hybrid membranes[23,24] have shown improved physicochemical properties such as oxidative stability, proton conductivity, water absorption, and so on.[6,25−34] The functionalization of sPEEK polymer with organic moieties such as benzimidazole, imidazole, or triazole[35,36] or also phthalocyanine dyes,[37,38] as well as polymeric blend with polyethylenimine[39] or polyaniline,[40] have also been reported to improve membrane microstructure, thermal properties, water uptake, and conductivity with respect to the pristine polymer. Recently, in order to improve proton conductivity under drastic humidity conditions (relative humidity, RH < 25%), we reported an investigation on composite membranes based on sPEEK and 5,10,15,20-tetra(4-pyridyl)porphyrin (TPyP), which retain the structural and morphological properties of the pure polymer.[41] Despite many reports dealing with the use of porphyrin systems in fuel cells technology as non-platinum group metal catalysts in oxygen reduction reaction (ORR),[42−45] to the best of our knowledge, no reports on the implication of porphyrin supramolecular systems to improve the performance of proton conducting membranes for PEFC application have been reported so far, except for similar systems based on sulfonated metal phtalocyanine.[37] Porphyrins are very versatile compounds whose chemical−physical properties can be tuned through a careful choice of peripheral substituent groups, which are also responsible for their aggregation state.[46] In this respect, the water-soluble tetranionic *meso*-tetrakis(4-sulfonatophenyl)-porphyrin (TPPS) received high attention due to its ability to self-assemble in J-aggregates.[47−53] In the past, we reported on the ability to easily tune porphyrin J-aggregates' optical features, using Nafion membranes as a confined environment to arrange and orient the chromophores.[54] Since Nafion is the most used polymer electrolyte membrane in PEFCs, also the role of the porphyrin aggregates into the proton conduction mechanism of the membranes has been investigated even if porphyrin release in the fuel cells' working conditions has been detected. sPEEK is a good candidate not only to overcome the operative Nafion limitations but also for the ability of its sulfonated groups to interact with the protonated central core of the porphyrin macrocycles so stabilizing the dyes into polymeric ionic domains.[6] Here, we report on the role of TPPS J-aggregates on the performance of the composite sPEEK based membranes at different porphyrin weight percentages (0.35−5 wt % TPPS/sPEEK). We anticipate that, on controlling the TPPS load, we successfully addressed tuning the porphyrin aggregation into the proton-conducting channels of the membranes. Thus, we obtained composite materials with peculiar behavior in terms of good proton conductivity, chemical stability, and fuel cells performance. To get better insight into the specific interaction responsible for the improved quality of the materials, we have conducted a detailed spectroscopic investigation and physical chemical characterizations of the composite membranes. Furthermore, electrochemical accelerated degradation test on PEFC single cell, simulating the typical operative conditions for portable applications, highlighted the improved stability of the composite membrane compared to that of the pristine sPEEK.

## RESULTS AND DISCUSSION

Porphyrin composite sPEEK membranes are prepared by casting the polymeric dispersion of sPEEK and TPPS at different weight percentages (wt %). The doctor-blade casting method was chosen to obtain the high porphyrin dispersion homogeneity and reproducibility of thickness on large scale. Our approach takes advantage of the occurrence of electrostatic interactions between the sulfonated functional groups of the poly(ether ether ketone) and the diacid form of TPPS porphyrin, which is well-known to be able to self-aggregate under specific acidic conditions and in confined microenvironments.[55−57] Indeed, in aqueous solution, these supramolecular structures are stabilized through a network of electrostatic and hydrogen-bonding interactions mainly involving the negatively charged sulfonate groups present in the periphery of the porphyrins and their positively charged inner nitrogen core. These aggregates are characterized by the occurrence of a sharp and consistently red-shifted B-band ($\Delta\lambda$ = ≥50 nm) with respect to the porphyrin free base together with an intense resonant light scattering signal at the red edge of the absorption band.[58] In the present investigation, to prepare the composite membranes, the TPPS filler (previously solubilized in the same solvent of the polymer) was added to the polymeric dispersion (10% in dimethylacetamide (DMAc)). The addition of the dye instantaneously induces a color change in the polymeric dispersion, which turns from slight yellow to dark green. This latter color is typical of TPPS acid species due to the protonation of the porphyrin central core ($pK_a$ 4.9 in water)[59] and/or to the full protonation of the sulfonated end groups of the macrocycles.[57] In order to better define the nature of the porphyrin species present in the mixture and to exclude the formation of preformed porphyrin aggregates, a spectroscopic characterization has been performed on the porphyrin/sPEEK dispersion in DMAc. The electronic spectrum recorded on the crude dispersion (see Supporting Information Figure S1) reveals the presence of two Soret bands centered at 420 and 450 nm ascribable to the porphyrin free base[60] and its diacid form, respectively. This is confirmed by the electronic spectra recorded on TPPS in DMAc with and without the addition of acid to the solution (see Figure S1). The light scattered by the samples is comparable to that of the neat solvents suggesting the absence in solution of porphyrin aggregates (data not shown). Therefore, the membrane preparation procedure can be divided into two steps: (i) casting, with the formation of porphyrin aggregates driven by weak intermolecular forces throughout the evaporation process, and (ii) postcasting, consisting of thermal and acid treatments carried out to


DOI: 10.1021/acsaem.8b00126
ACS Appl. Energy Mater. 2018, 1, 1664−1673

stabilize, purify, and enhance the wettability of the prepared material. Transparent green membranes of homogeneous thickness ranging from 40 to 50 $\mu$m have been obtained at different porphyrin/sPEEK load. Independently from thickness and TPPS load, the embedded dyes in the membranes exhibit good stability and chemical resistance to both thermal annealing and acid treatments, as shown by the unchanged spectroscopic features. The extinction spectra of the membranes with different porphyrin load after thermal and acidic treatments are reported in Figure 1. Furthermore, the

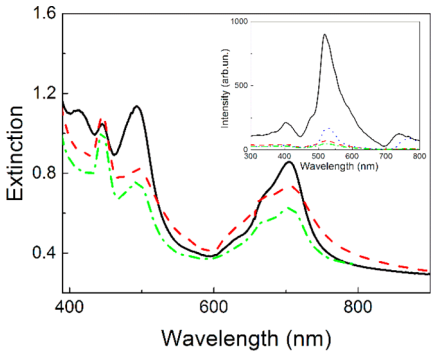


**Figure 1.** Extinction spectra (inset, corresponding RLS spectra) of composite TPPS/sPEEK membranes recast from DMAc, $T$ = 298 K: [TPPS] = 0.35 wt % (green dashed−dotted line), 0.77 wt % (black solid line), 1.5 wt % (red dashed line), and 5 wt % (blue dotted line). Due to the high extinction coefficient of the dye, the electronic spectra of the 5 wt % TPPS/sPEEK membrane has not been reported as out of the instrument detection upper limits.

composite membranes remained stable in aqueous solution and no release of porphyrins was observed even after months (see Figure S2). The electronic spectra (in the range 0.35−1.5 wt %) show the presence of a Soret band at 444 nm due to the diacid porphyrin species accompanied by various Q-bands in the range 500−700 nm and a band at about 494 nm, ascribable to the porphyrin J-aggregates. The presence of these species, in which porphyrins are strongly electronically coupled, is confirmed by a very intense resonant peak in the light scattering spectra (inset of Figure 1), much more intense for the 0.77 wt % sample where J-aggregates are the predominant species in the extinction spectra.

The spectroscopic features can be explained in terms of the Frenkel exciton model for electronic coupled porphyrins organized in a rod-like structure.[61] In the porphyrin load range 0.35−1.5 wt %, the composite membranes display fluorescence emission (Figure 2) with a main band component centered in the range 650−680 nm and a weaker band between 710 and 740 nm, whose position and intensity are dependent on the porphyrin load. For all these samples, the excitation profile, reported in the inset of Figure 2, matches the extinction spectra of the diacid species. For the 5 wt % TPPS/sPEEK sample the emission spectrum is characterized by a main component band, red-shifted with respect to the main band of the other samples, at about 754 nm. In general, for all the samples the complexity of the fluorescence emission spectra and the variability of the band position suggest the presence of more than a single emissive species.

In order to test the stability of the J-aggregates into the membranes, we performed a detailed spectroscopic investigation on the 0.77 wt % sample. The spectroscopic features of composite membranes remain unchanged after immersion in

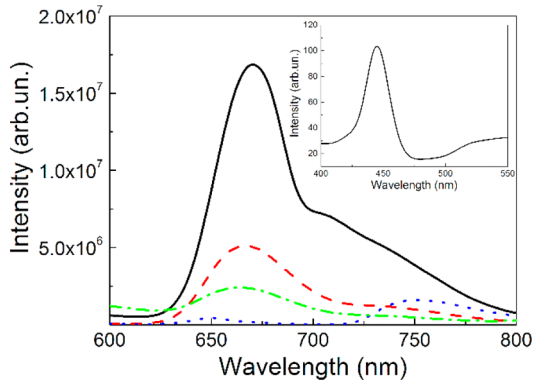


**Figure 2.** Fluorescence emission spectra (inset, typical excitation spectrum) of composite TPPS/sPEEK membranes recast from DMAc, $T$ = 298 K: [TPPS] = 0.35 wt % (green dashed−dotted line), 0.77 wt % (black line), 1.5 wt % (red dashed line), and 5 wt % (blue dotted line). $\lambda_{ex}$ = 450 nm; $\lambda_{em.}$= 660 nm.

highly acid media (12 M HCl; see Figure S3). On the contrary, in bulk aqueous solutions, TPPS J-aggregates remain stable up to 4 M HCl concentration. A further increase of acidic concentration induces disaggregation for protonation of the sulfonated end groups.[57] Indeed, in the composite membranes, the observed stability is a clear indication of their location into sPEEK hydrophilic channels. These latter are responsible for the swelling behavior and water and proton transport coefficients, as well as the electroosmotic drag and water permeation of the native sPEEK membranes.[5] To further confirm this hypothesis, we dipped the composite membranes in methanol solution, in which their swelling and filler release ability is well-known.[17] The absorbance spectrum (see Figure S4) recorded on the alcohol solution shows the presence of a main band centered at 438 nm and a minor component at 416 nm ascribable to TPPS in its monomeric diacid and free base forms,[62] respectively, thus suggesting a complete release of the dyes in a couple of days. Moreover, to check the proton exchange process, we dipped the composite membranes into alkaline solutions (1 M NaOH) and instantaneously we observed a color change from green to red. This evidence is ascribable to porphyrin disaggregation, as confirmed by the disappearance in the extinction spectrum (Figure 3) of the typical TPPS J-aggregate band together with the appearance of

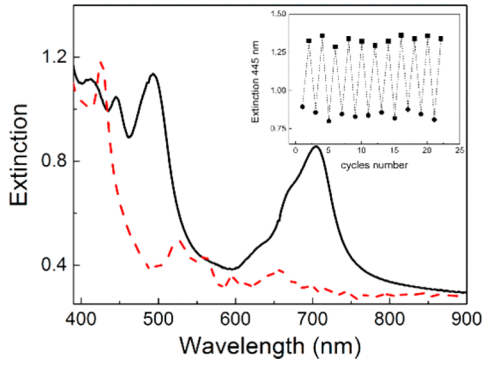


**Figure 3.** Extinction spectra (inset, extinction value at 445 nm after cyclic dipping into acidic $H_2SO_4$ 0.5 M and alkaline NaOH, 1 M solutions) of composite TPPS/sPEEK membranes recast from DMAc, $T$ = 298 K: [TPPS] = 0.77 wt % (solid line); after dipping in NaOH 1 M solutions (red dashed line).


DOI: 10.1021/acsaem.8b00126
ACS Appl. Energy Mater. 2018, 1, 1664−1673

**Table 1. Fluorescence Lifetimes (ns) and Relative Amplitude (%), for sPEEK/TPPS Membranes with Different Porphyrin Loads (wt % TPPS/sPEEK) at 293 K**

| TPPS/sPEEK, wt % | $\tau_1$ | $\tau_2$ | $\tau_3$ | $A_1$ | $A_2$ | $A_3$ |
|---|---|---|---|---|---|---|
| 0.35[a] | 5.1 ± 0.04 | 2.6 ± 0.3 | 0.4 ± 0.02 | 61 | 21 | 18 |
| 0.77[a] | 4.9 ± 0.05 | 1.93 ± 0.1 | 0.33 ± 0.02 | 46 | 26 | 28 |
| 1.5[a] | 5.3 ± 0.02 | 1.82 ± 0.05 | 0.06 ± 0.02 | 40 | 23 | 37 |
| 5[b] | 5.14 ± 0.05 | 1.84 ± 0.1 | 0.2 ± 0.01 | 26 | 28 | 46 |
| 0.77[c] | 11.2 ± 0.02 | 1.89 ± 0.05 | | 82 | 18 | |

[a]Emission at 664 nm. [b]Emission at 750 nm. [c]After treatment in 1 M NaOH.

a new Soret band centered at 426 nm accompanied by four Q-bands centered at 526, 564, 598, and 660 nm, respectively. The number of Q-bands of the new species is a clear indication of a $D_{2h}$ geometry for the porphyrin ring, pointing out the occurrence of the porphyrin core deprotonation. This species is stable for prolonged immersion in alkaline solutions where no porphyrin release has been observed. This finding confirms, once again, the location of the porphyrin species into the sPEEK ionic domains not subjected to swell in the investigated experimental conditions. Furthermore, the emission spectrum of the sample shows the presence of two bands centered at 655 and 718 nm, respectively (see Figure S5). It has been reported in literature that, in aqueous solution, at pH = 9.0 TPPS is present as a monomeric tetra-anionic species able to form a noncovalent dimer in the presence of potassium ion and crown ether.[63,64] Protonation and consequently porphyrin aggregation can be restored by dipping the composite membrane into acid solution (0.5 M $H_2SO_4$). It is worth noting that protonation/deprotonation and the subsequent porphyrin aggregation/disaggregation processes are fast and reversible upon repetitive cycling of the pH conditions (inset of Figure 3).

To get better insights into the nature of the porphyrin located into the sPEEK ionic domains, time-resolved fluorescence measurements, at room temperature, have been performed on all the samples. The lifetime values with their relative amplitudes are collected in Table 1. The emission decays for the aggregated samples show a triexponential behavior: (i) a long lifetime value of about 5 ns, which is prevalent in the porphyrin load range 0.35−1.5 wt % TPPS/sPEEK (relative amplitude of about 45%); (ii) a shorter one of about 1.9 ns, whose relative amplitude is about 25% for all the samples; and (iii) a very short lifetime value of about 0.2 ns, which is the prevalent emitting species for 5 wt % TPPS/sPEEK (relative amplitude of about 46%). In good agreement with the data already reported for TPPS species in aqueous solution in the presence of crown ether systems[63,64] or confined in microemulsions,[56] the long lifetime value can be assigned to the monomeric form of the diacid TPPS porphyrin. The intermediate-living species (1.9 ns) can be ascribed to a J-dimer and the shortest-living species to porphyrin J-aggregates. Indeed, in our systems, for all the porphyrin species, we found slightly increased values with respect to those reported in literature. This evidence can be due to the confinement effect of the fluorophores in the sPEEK ionic domains where the solvent quenching effect is reduced.

The emission decay on 0.77 wt % sample after alkaline treatment exhibits a biexponential behavior with a long lifetime value of about 11 ns and relative amplitude of about 82%, together with a shorter one of about 1.9 ns (data collected in Table 1). On comparing these data with those already reported for TPPS species in alkaline aqueous solutions, it is possible to ascribe the long- and short-living species to the porphyrin in its tetra-anionic monomeric and dimeric forms, respectively.[63,64] The nanostructure of the composite membranes has been investigated using SAXS. All the samples show the characteristic ionomer peak usually observed in ionomers, indicating the presence of phase separation at the nanoscale (see Figure 4).

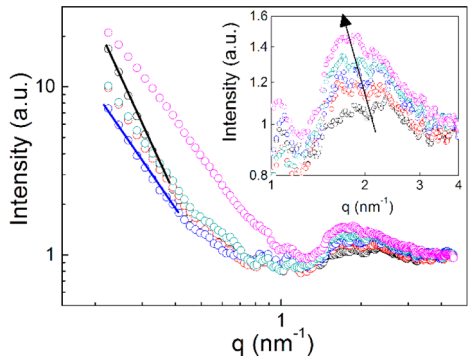


**Figure 4.** SAXS profiles of composite TPPS/sPEEK membranes recast from DMAc equilibrated at room humidity: pristine membrane (empty black circles); [TPPS] = 0.35 wt % (empty red circles), 0.77 wt % (empty blue circles), 1.5 wt % (empty green circles), and 5 wt % (empty purple circles). Black and blue lines indicate $q^{-4}$ and $q^{-2}$ power laws, respectively. Inset: enlarged view of the ionomer peak.

The ionomer peak of the recast sPEEK membrane is located at about $q^* = 2$ nm$^{-1}$. According to Bragg's law, the characteristic dimension of the ionic domains of sPEEK is $2\pi/q^* = 3.1$ nm. The ionomer peak gradually increases in intensity and shifts toward smaller $q$-values (i.e., larger dimensions) when increasing the porphyrin load. The characteristic dimension of the ionic domains for the 5 wt % TPPS/sPEEK composite membrane is 3.7 nm. These values are larger than what was reported for pristine sPEEK cast from DMAc, with both lower[17] and the same degree of sulfonation.[65] The increase in intensity and the shift of the ionomer peak toward lower angles (see inset of Figure 4) confirm that the porphyrins, in their different forms, are predominantly located inside the ionic domains. The presence of the porphyrins also has an influence on the membrane structure at larger length scales. The SAXS curve for the sPEEK membrane exhibits a $q^{-4}$ slope at the lowest angles ($q < 0.5$ nm$^{-1}$), indicating large-scale heterogeneities of the spatial distribution of the ionic domains often reported for ionomers.[66] In contrast, the composite membranes in the 0.35−1.5 wt % range show a slope of about $q^{-2}$ suggesting a reorganization of the ionic domains (in terms of connectivity and spatial distribution) toward a lamellar-like morphology.[67] We believe that this reorganization is due to the supramolecular interaction between sPEEK and the porphyrins in their different forms. The scattering at low angles is significantly increased for the 5 wt % sample.


DOI: 10.1021/acsaem.8b00126
ACS Appl. Energy Mater. 2018, 1, 1664−1673

This extra scattering contribution is due to the presence of a significant fraction of J-aggregates, as suggested by the time-resolved fluorescence data aforementioned. SAXS data are in agreement with a rod-like structure model showing a cross-sectional dimension of about 2.5 nm (see Figure S6). Based on collected data, we reported in Scheme 1 a hypothetical model

**Scheme 1. Hypothetical Model for Composite TPPS/sPEEK Membranes**

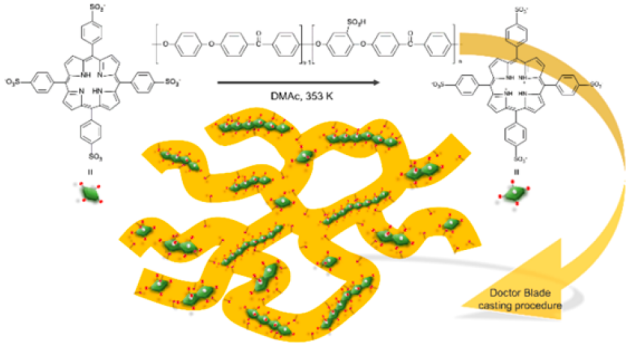


that takes into account the stabilization of the TPPS and the supramolecular growth of the J-aggregates into the polymeric ionic domains. This is due to hydrogen bonds and electrostatic interactions acting between the negatively charged sulfonated groups of sPEEK polymer and positively charged porphyrin core, which allow the anchoring of the dyes and the formation of a supramolecular network with a rod-like structure. It is worth noticing that, as reported in literature, in TPPS J-aggregates the monomeric porphyrin units stack side-by-side in a variety of structural morphologies depending on the growing experimental conditions.[68] Previous X-ray investigations demonstrated, at high porphyrin concentration, the arrangement of the dyes in a rod-like structure whose length decreases on increasing the monomer concentration.[69] SAXS experiments carried out in aqueous solution pointed to the presence of a hollow cylinder with shell thickness compatible to the porphyrin molecule dimension.[70,68] X-ray and electron diffraction investigations have demonstrated the existence of a basic sheet-like architecture able to form multilayers through interactions of their lateral meso-substituents.[71] The presence of monomer, dimer, and aggregated TPPS inside the ionic domains influences not only the structure but also the physical–chemical properties of the membrane.

In particular, the ion-exchange capacity of the membranes slightly increases with the minimum amount of TPPS introduced (0.35 wt %). The ion-exchange capacity (IEC) data are collected in Table 2. In this experimental condition, as suggested by time-resolved fluorescence data, TPPS is mainly distributed into the polymeric matrix in its monomeric form. This allows for an increase of the sulfonic groups responsible for the enhanced ion-exchange capacity. On increasing the porphyrin load (0.77–5 wt %) IEC remains quite constant. This behavior is due to the formation of J-aggregates' supramolecular network that involves the sulfonated groups of both the polymer and the porphyrin. We suggest that the IEC value is a compromise among the free proton ions, those involved in the interactions between the sulfonic groups of the polymer and the TPPS, and those responsible for the TPPS stacking in the J-aggregates. In order to evaluate the water arrangement in the membranes, a comparison among water uptake ($W_{up}$), area ($\Delta A$%), and thickness ($\Delta t$%) dimensional variations was carried out, as reported in Figure 5 and Table 2.

**Table 2. Chemical Physical Parameters for Composite TPPS/sPEEK Membranes with Different Porphyrin Loads (wt % TPPS/sPEEK), $T$ = 303 K**

| sample | TPPS loading, % | $W_{up}$, % | IEC, mequiv/g | $\sigma$, mS/cm |
|---|---|---|---|---|
| sPEEK | | 46 | 1.80 | 42 |
| 0.35 wt % TPPS/sPEEK | 0.35 | 46 | 2.01 | 48 |
| 0.77 wt % TPPS/sPEEK | 0.77 | 51 | 1.97 | 53 |
| 1.5 wt % TPPS/sPEEK | 1.5 | 49 | 2.00 | 43 |
| 5 wt % TPPS/sPEEK | 5 | 50 | 1.99 | 38 |

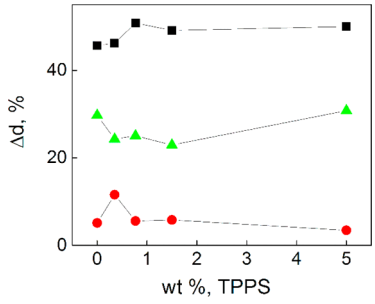


**Figure 5.** Water uptake and dimensional variations of membranes as a function of TPPS%–$W_{up}$% (black filled squares), $\Delta t$% (red filled circles), and $\Delta A$% (green filled triangles).

The water uptake carried out at 303 K in liquid water is the same as that of the pristine polymer for the 0.35 wt % sample while it increases on increasing the TPPS load, in line with hydration ability of the sulfonated porphyrins. It is visible that the introduction of TPPS (0.35 wt %) increases the $\Delta t$%, reducing the $\Delta A$%, suggesting a preferential distribution of the water occurs. On the contrary, an increase of the TPPS amount (0.77 wt %) induces an increase of the $W_{up}$, a reduction of the $\Delta t$% but not a corresponding increase of $\Delta A$%. This behavior suggests that the water could be mainly located into the hydrophilic channels and not in the entire polymeric matrix. In particular, we are inclined to think that, the presence of "voids" into the growing J-aggregates' structures allows increasing the water uptake without inducing any membrane's dimensional variations. A further addition of TPPS (1.5 wt %) does not affect the water distribution differently from higher porphyrin load (5 wt %) for which $W_{up}$ and $\Delta t$% remain quite unaltered while $\Delta A$% increases.

In line with time-resolved fluorescence and SAXS data, this effect should be related to a larger amount of aggregates with respect to monomeric or dimeric porphyrins. This finding suggests an almost complete occupancy of the hydrophilic channels so inducing a water distribution between them and the entire polymeric matrix. Finally, we explored the electrochemical performances of the porphyrin/sPEEK composite membranes. Interestingly, TPPS leads to an increment of the proton conductivity with a maximum value for 0.77 wt % and a minimum for 5 wt % sample, respectively. This behavior is also in accordance with the IEC and $W_{up}$ data (Table 2), indicating that the water distribution plays a key role in the proton conductivity. The proton conductivity of sPEEK composite membranes, with sulfonation degree comparable to our systems, measured in similar operative conditions is generally


DOI: 10.1021/acsaem.8b00126
ACS Appl. Energy Mater. 2018, 1, 1664–1673

lower than that reported in this work (53 mS/cm for 0.77 wt % TPPS/sPEEK) except when a proton conductor is used.[72−82] This result evidences the advantage of the introduction in the membranes of TPPS porphyrin, which plays a key role in the proton conductivity mechanism. To verify the electrochemical trend in a fuel cell, preliminary tests were carried out at 303 K and ambient pressure. Fuel cell tests were carried out to feign the real application, with operative conditions of 30 °C, ambient pressure, dry hydrogen simulating a feeding by a tank, and fully humidified air simulating a cathodic air-breathing operation comprising the water production. The *I*−*V* curves comparison among all the samples are reported in Figure 6. All

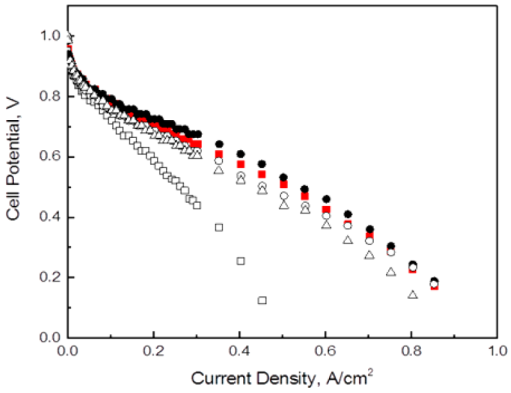


**Figure 6.** *I* vs *V* curves at 303 K, 1 bar absolute, dry $H_2$, and 100% RH air for sPEEK: pristine (red filled squares); [TPPS] = 0.35 wt % (black empty squares), 0.77 wt % (black filled circles), 1.5 wt % (black empty triangles), and 5 wt % (black empty circles).

the tested membranes display a good value of OCV (about 1 V) indicating a dense structure of the samples. Moreover, the composite membranes show comparable or slightly lower performance than pristine membrane, with a progressive decay with different TPPS loadings. It is worth noting the best performance was achieved with the 0.77 wt % sample, similarly to what was observed for proton conductivity. In terms of power density calculated at 0.5 A/cm$^2$, the 0.35 wt % sample is the lowest one because at this selected current density it reaches its limiting current density. The 1.5 and 5 wt % samples exhibit similar performance (237 and 221 mW/cm$^2$, respectively), but lower than the pristine polymer (256 mW/cm$^2$) and the 0.77 wt % sample (267 mW/cm$^2$); see Figure S7. The power density trend observed in our samples is not totally in agreement with the proton conductivity data. This could be explained considering that different sections of membranes are investigated (through the plane for *I*−*V* curves and in plane for $\sigma$), indicating a certain degree of anisotropy of the material.[83] Indeed, the investigated section is irrelevant when the water uptaken is mainly distributed in the hydrophilic channels uniformly in the three dimensions (0.77 wt % sample). On the contrary, it becomes relevant if water is preferentially distributed in the area or in the thickness (0.35 and 5 wt % samples). Therefore, we can assume a lower degree of anisotropy for composite membrane with 0.77 wt % porphyrin load.

On these bases and considering that the best performance was reached for the 0.77 wt % sample and pristine sPEEK membrane, these samples were selected to perform further electrochemical tests. In particular, an accelerated degradation test (ADT) was carried out to undergo the membranes to swelling/deswelling process, cycling the current between 0.2 and 0.8 A/cm$^2$ and monitoring the cell voltage during the time (Figure 7). The temperature, pressure, and relative humidity of

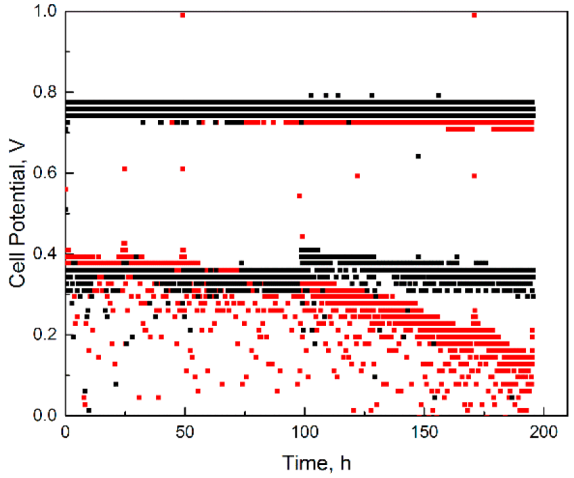


**Figure 7.** Accelerated degradation test at 303 K, 1 bar absolute, dry $H_2$, and 100% RH air for sPEEK: pristine (red filled circles); 0.77 wt % TPPS/sPEEK (black filled circles).

gases were selected to simulate the real operative conditions of a portable device fed by a hydrogen tank. As evident, a cell potential decay was recorded for pristine sPEEK after 100 h of operation while a good stability was maintained for the 0.77 wt % composite sample for about 200 h and afterward the test was voluntarily stopped. In fact, the potential decay recorded between 0 and 100 h is similar for the two membranes and corresponds to 4.1 and 3.3 mV/h for sPEEK and 0.77 wt % TPPS/sPEEK, respectively. On the contrary, between 100 and 200 h of operation a further decay was recorded for sPEEK (2.1 mV/h) while quasi stable potential was maintained during this time for the composite membrane (0.3 mV/h). This behavior could be justified by taking into account a different water distribution in the two investigated membranes. In accordance to the dimensional variations, the distribution of water in pristine membrane is mainly located in the area, so the swelling/deswelling process affects the mechanical properties causing a detrimental effect on performance stability. On the contrary, the 0.77 wt % sample, which is less sensitive to the dimensional variations, shows a better stability during the ADT. The polarization curves carried out at the beginning and at the end of ADT (Figure 8) show that there was no evident performance variation for 0.77 wt % TPPS/sPEEK while a slight performance reduction was recorded for the pristine membrane, in particular in the high current density area of the curve (see Figure S8).

As already reported, the polymer structural arrangement that is directly correlated to the mechanical properties of the membranes plays a key role.[84] In fact, the presence of TPPS induces a reorganization of polymer chains in lamellar-like form, implying a more crystalline and organized structure thus leading to a more robust and resistant polymeric matrix able to maintain its stability during ADT. The SEM images reported in Figure S9 confirm a different morphology for the composite and pristine membranes, respectively. It is important to notice that one of the targets of the DoE is the durability of the system with an ultimate target of 5000 h under operation.[85] In this framework, obtaining composite membranes with improved


DOI: 10.1021/acsaem.8b00126
ACS Appl. Energy Mater. 2018, 1, 1664−1673

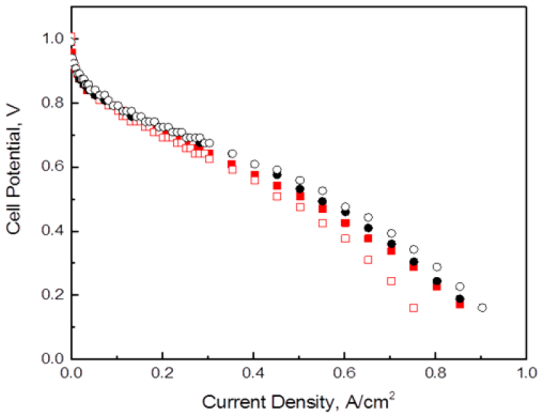


**Figure 8.** *I* vs *V* curves at 303 K, 1 bar absolute, dry $H_2$, and 100% RH for sPEEK: pristine at beginning (red filled squares) and at the end of ADT (red empty squares); 0.77 wt % TPPS/sPEEK at beginning (black filled circles) and at the end of ADT (black empty circles).

durability is a key aspect in manufacturing new materials for fuel cell applications. To the best of our knowledge, no reports on membranes' durability test or ADT in real operative conditions for portable applications have been reported so far.

## EXPERIMENTAL SECTION

**Polymer Sulfonation.** Polymer sulfonation was carried out, according to a standardized procedure,[6] in concentrated sulfuric acid in order to obtain a 65% sulfonated poly(ether ether ketone) (Victrex PF450).

**Membrane Preparation.** sPEEK membranes were prepared with a doctor-blade technique after a dissolution of the polymer in dimethylacetamide (DMAc) according to an already reported standardized procedure.[6] Composite TPPS/sPEEK membranes were prepared by adding to the sulfonated polymer solution different weight percentages 0.35, 0.77, 1.5, and 5 wt % of *meso*-tetrakis(4-sulfonatophenyl)porphyrin. The latter was purchased from Aldrich Co. as tetrasodium salt and used without further purification. All the membranes were dried at 353 K for 3 h and successively treated at 393 K for 16 h. An acid treatment in 1 M $H_2SO_4$ at 333 K was carried out to purify the membranes of any residual solvent and to activate groups for proton ion exchange and the coordination of water molecules.

**Instruments.** UV/vis spectra were performed on a Hewlett-Packard model 8453 diode array spectrophotometer. Static and time-resolved fluorescence emission measurements were performed on a Jobin Yvon-Spex Fluoromax 4 spectrofluorimeter using time-correlated single-photon counting technique. A NanoLED ($\lambda$ = 390 nm) has been used as excitation source. Emission spectra were not corrected for the absorbance of the samples.

Resonance light scattering (RLS) experiments were performed on a Jasco model FP-750 spectrofluorimeter, adopting a synchronous scan protocol with a right angle geometry.[58] RLS spectra were not corrected for the inner-filter effect of the samples.[86]

Small-angle X-ray scattering experiments were performed at the BM26B beamline DUBBLE at the ESRF, Grenoble, France.[85,87] An X-ray radiation with wavelength of 1.033 Å and a sample-to-detector distance of 2 m were used. SAXS images were collected using a high sensitivity, noiseless Pilatus 1 M detector with pixel dimensions of 172$\mu$m × 172 $\mu$m. The probed angular range was calibrated using the known position of diffraction rings from a standard silver behenate powder sample. Radial averaging of the images was performed in order to obtain the 1D SAXS profiles. Corrections for incident beam intensity, sample absorption, and air background scattering were applied before performing the radial averaging operation.

The IEC (mequiv of $SO_3H$/mg) was calculated through an acid–base titration following the experimental procedure described elsewhere.[6] IEC is calculated using the formula

$$\mathrm{IEC_m} = (V_{\mathrm{tit}}[\mathrm{M}])/m_{\mathrm{dry}}$$

where $V_{tit}$ = titrant volume (mL), [M] = titrant molarity, and $m_{dry}$ = dry mass of the sample (g);

The water uptake of the membranes ($W_{up}$, %) was calculated from the difference in weight between the dried and the wet sample.

$$W_{\mathrm{up}}/\% = \frac{(m_{\mathrm{wet}} - m_{\mathrm{dry}})}{m_{\mathrm{dry}}} \times 100$$

The wet mass ($m_{wet}$) is determined after immersion of the sample in distilled water at room temperature for 24 h, while, for the dry mass ($m_{dry}$), the sample is dried in a vacuum oven at 353 K for 2 h.

The proton conductivity was measured in the in plane section of the sample with a four-probe technique, DC current, at 303 K and full humidification (100% RH) using a commercial cell (Bekktech). The proton conductivity was calculated using the equation

$$\sigma = L/RWT$$

where $L$ = 0.425 cm, the constant distance between the two Pt electrodes; $R$ = resistance (Ω); $W$ = sample width (cm); and $T$ = sample thickness (cm).

**Fuel Cell Tests.** Homemade electrodes were prepared by spraying the catalytic ink onto a commercial gas diffusion layer Sigracet-24BC (SGL group).[88] The catalytic ink was obtained by mixing 50% Pt/C (Alfa Aesar) with a 33 wt % dry Nafion (5 wt % hydroalcoholic solution) with an EW of 1100 g/mol. For catalyst layer preparation, 20 wt % ammonium carbonate was used as a pore-former. A Pt loading of 0.5 mg $cm^2$ for both the anode and the cathode sides was used. Membrane and electrodes were directly assembled in the single cell, tightened at 10 N m, to obtain MEAs (membrane–electrodes assemblies).

Fuel cell tests, in terms of polarization curves, were carried out in a commercial 25 $cm^2$ single cell at 303 K, dry $H_2$/100% RH air at 1 abs. The gas fluxes were fixed at 1.5 and 2 times the stoichiometry at the current work for hydrogen and air, respectively. Accelerated degradation tests (ADT) were performed by cycling the current density between 0.2 and 0.8 A/$cm^2$. Every cycle consists of two steps of 10 min at the fixed current density, so each cycle had a duration of 20 min. The cell voltage was monitored during the time. The ADT was carried out for 200 h.

## CONCLUSIONS

Highly homogeneous TPPS porphyrin/sPEEK composite membranes have been prepared by doctor-blade casting procedure of the polymeric dispersion of sPEEK and TPPS at different weight percentages. The produced membranes showed high stability and are promising for fuel cell applications. Our approach takes advantage of the occurrence of electrostatic interactions between the sulfonated functional groups of the poly(ether ether ketone) and the diacid form of TPPS porphyrin, which self-assembles into J-aggregates. Static and time-resolved spectroscopic characterization show, unambiguously, the presence of TPPS in its monomeric, dimeric, and aggregated forms into the membrane ionic domains at different percentages as a function of porphyrin load. SAXS analysis shows that the addition of TPPS into the sPEEK membrane plays a key role in structuring, at nanoscale, the polymeric ionic domains, responsible of performance of the material in PEFC devices. Controlling the porphyrin load and consequently the distribution between monomeric and aggregated species, we succeeded in modulating the chemical stability, the proton conductivity, and the fuel cells performance. In particular, we observed for the 0.77 wt % sample the best performance (267 mW/$cm^2$ at 0.5 A/$cm^2$). A good balance between monomeric and aggregated porphyrin results in an enhanced proton membrane conductivity, due to the extra


DOI: 10.1021/acsaem.8b00126
ACS Appl. Energy Mater. 2018, 1, 1664–1673

sulfonated groups of the porphyrin free base, together with an improvement of the mechanical properties related to the polymer structural rearrangement due to the presence of the aggregates. Electrochemical degradation investigations in a PEFC single cell, simulating the operative conditions typical for portable applications, have been carried out at this specific porphyrin load. We successfully addressed the key problem of sPEEK membranes stability, highlighting, during the accelerated degradation test, that no decay of cell potential was recorded for composite membrane even after a prolonged time in comparison with the pristine sPEEK membrane taken as reference.

## ■ ASSOCIATED CONTENT

### Supporting Information

The Supporting Information is available free of charge on the ACS Publications website at DOI: 10.1021/acsaem.8b00126.

Absorption spectra, membrane stabilities, fluorescence emission spectrum, SAXS on composite membrane, molar and swelling ratios, power density curves, and SEM images (PDF)

## ■ AUTHOR INFORMATION


### Corresponding Author

*E-mail: castriciano@pa.ismn.cnr.it.

### ORCID

Massimiliano Gaeta: 0000-0001-8521-4195
Giuseppe Portale: 0000-0002-4903-3159
Maria Angela Castriciano: 0000-0002-1514-8820


### Notes

The authors declare no competing financial interest.

## ■ ACKNOWLEDGMENTS

We thank CNR for financial support "Nanomateriali e nanotecnologie per lo sviluppo sostenibile ed il patrimonio culturale" (CUP: G78B14000100006, 1/2012, grant to M.G.) and Prof. L. Monsù Scolaro (UniME) for useful discussion.

## ■ ABBREVIATIONS

ADT = accelerated degradation tests.
DMAc = dimethylacetamide
DoE = U.S. Department of Energy
IEC = ion-exchange capacity
MEAs = membrane−electrodes assemblies
RLS = resonance light scattering
SAXS = small-angle X-ray scattering
sPEEK = sulfonated poly(ether ether ketone)
TPPS = meso-tetrakis(4-sulfonatophenyl)porphyrin
$W_{up}$ = water uptake

## ■ REFERENCES


(1) Scofield, M. E.; Liu, H. Q.; Wong, S. S. A Concise Guide to Sustainable Pefcs: Recent Advances in Improving Both Oxygen Reduction Catalysts and Proton Exchange Membranes. *Chem. Soc. Rev.* **2015**, *44*, 5836−5860.

(2) Kundu, P. P.; Dutta, K. Hydrogen Fuel Cells for Portable Applications. *Compendium of Hydrogen Energy: Hydrogen Use, Safety and the Hydrogen Economy* Woodhead, Elsevier: Amsterdam, 2015; Vol. *4*, Chapter 6, pp 111−131, DOI: 10.1016/B978-1-78242-364-5.00006-3.

(3) Heinzel, A.; Wartmann, J.; Dura, G.; Helm, P. Portable Fuel Cells. *Hydrogen and Fuel Cell: Technologies and Market Perspectives*; Springer: Berlin, Heidelberg, 2016.

(4) *DOE Technical Targets for Fuel Cell Systems for Portable Power and Auxilliary Power Applications*, https://Energy.Gov/Eere/Fuelcells/Doe-Technical-Targets-Fuel-Cell-Systems-Portable-Power-and-Auxiliary-Power.

(5) Kreuer, K. D. On the Development of Proton Conducting Polymer Membranes for Hydrogen and Methanol Fuel Cells. *J. Membr. Sci.* **2001**, *185*, 29−39.

(6) Carbone, A.; Pedicini, R.; Sacca, A.; Gatto, I.; Passalacqua, E. Composite S-Peek Membranes for Medium Temperature Polymer Electrolyte Fuel Cells. *J. Power Sources* **2008**, *178*, 661−666.

(7) Poppe, D.; Frey, H.; Kreuer, K. D.; Heinzel, A.; Mülhaupt, R. Carboxylated and Sulfonated Poly(Arylene-Co-Arylene Sulfone)S: Thermostable Polyelectrolytes for Fuel Cell Applications. *Macromolecules* **2002**, *35*, 7936−7941.

(8) Zhang, Y.; Li, C.; Liu, X.; Yang, Z.; Dong, J.; Liu, Y.; Cai, W.; Cheng, H. Fabrication of a Polymer Electrolyte Membrane with Uneven Side Chains for Enhancing Proton Conductivity. *RSC Adv.* **2016**, *6*, 79593−79601.

(9) Borup, R.; Meyers, J.; Pivovar, B.; Kim, Y. S.; Mukundan, R.; Garland, N.; Myers, D.; Wilson, M.; Garzon, F.; Wood, D.; Zelenay, P.; More, K.; Stroh, K.; Zawodzinski, T.; Boncella, J.; McGrath, J. E.; Inaba, M.; Miyatake, K.; Hori, M.; Ota, K.; Ogumi, Z.; Miyata, S.; Nishikata, A.; Siroma, Z.; Uchimoto, Y.; Yasuda, K.; Kimijima, K.-i.; Iwashita, N. Scientific Aspects of Polymer Electrolyte Fuel Cell Durability and Degradation. *Chem. Rev.* **2007**, *107*, 3904−3951.

(10) Hamada, T.; Hasegawa, S.; Fukasawa, H.; Sawada, S.-i.; Koshikawa, H.; Miyashita, A.; Maekawa, Y. Poly(Ether Ether Ketone) (Peek)-Based Graft-Type Polymer Electrolyte Membranes Having High Crystallinity for High Conducting and Mechanical Properties under Various Humidified Conditions. *J. Mater. Chem. A* **2015**, *3*, 20983−20991.

(11) Iulianelli, A.; Basile, A. Sulfonated Peek-Based Polymers in Pemfc and Dmfc Applications: A Review. *Int. J. Hydrogen Energy* **2012**, *37*, 15241−15255.

(12) Liu, B. J.; Robertson, G. P.; Kim, D. S.; Guiver, M. D.; Hu, W.; Jiang, Z. H. Aromatic Poly(Ether Ketone)S with Pendant Sulfonic Acid Phenyl Groups Prepared by a Mild Sulfonation Method for Proton Exchange Membranes. *Macromolecules* **2007**, *40*, 1934−1944.

(13) Seesukphronrarak, S.; Ohira, A. Novel Highly Proton Conductive Sulfonated Poly(P-Phenylene) from 2,5-Dichloro-4-(Phenoxypropyl)Benzophenone as Proton Exchange Membranes for Fuel Cell Applications. *Chem. Commun.* **2009**, 4744−4746.

(14) Zhang, X.; Sheng, L.; Hayakawa, T.; Ueda, M.; Higashihara, T. Polymer Electrolyte Membranes Based on Poly(Phenylene Ether)S with Sulfonic Acid Via Long Alkyl Side Chains. *J. Mater. Chem. A* **2013**, *1*, 11389−11396.

(15) Yee, R. S. L.; Rozendal, R. A.; Zhang, K.; Ladewig, B. P. Cost Effective Cation Exchange Membranes: A Review. *Chemical Engineering Research & Design* **2012**, *90*, 950−959.

(16) Carbone, A.; Pedicini, R.; Portale, G.; Longo, A.; D'Ilario, L.; Passalacqua, E. Sulphonated Poly(Ether Ether Ketone) Membranes for Fuel Cell Application: Thermal and Structural Characterisation. *J. Power Sources* **2006**, *163*, 18−26.

(17) Portale, G.; Carbone, A.; Martinelli, A.; Passalacqua, E. Microstructure, State of Water and Proton Conductivity of Sulfonated Poly(Ether Ether Ketone). *Solid State Ionics* **2013**, *252*, 62−67.

(18) Gebel, G. Structure of Membranes for Fuel Cells: Sans and Saxs Analyses of Sulfonated Peek Membranes and Solutions. *Macromolecules* **2013**, *46*, 6057−6066.

(19) Carbone, A.; Gatto, I.; Ohira, A.; Wu, L. B.; Passalacqua, E. Influence of Post-Casting Treatments on Sulphonated Polyether-etherketone Composite Membranes. *J. Power Sources* **2010**, *195*, 6037−6042.

(20) Delhorbe, V.; Cailleteau, C.; Chikh, L.; Guillermo, A.; Gebel, G.; Morin, A.; Fichet, O. Influence of the Membrane Treatment on




DOI: 10.1021/acsaem.8b00126
*ACS Appl. Energy Mater.* 2018, 1, 1664−1673

Structure and Properties of Sulfonated Poly(Etheretherketone) Semi-Interpenetrating Polymer Network. *J. Membr. Sci.* **2013**, *427*, 283−292.
(21) Inan, T. Y.; Dogan, H.; Unveren, E. E.; Eker, E. Sulfonated Peek and Fluorinated Polymer Based Blends for Fuel Cell Applications: Investigation of the Effect of Type and Molecular Weight of the Fluorinated Polymers on the Membrane's Properties. *Int. J. Hydrogen Energy* **2010**, *35*, 12038−12053.
(22) Li, Y.; He, G.; Wang, S.; Yu, S.; Pan, F.; Wu, H.; Jiang, Z. Recent Advances in the Fabrication of Advanced Composite Membranes. *J. Mater. Chem. A* **2013**, *1*, 10058−10077.
(23) Di Vona, M. L.; Marani, D.; D'Ottavi, C.; Trombetta, M.; Traversa, E.; Beurroies, I.; Knauth, P.; Licoccia, S. A Simple New Route to Covalent Organic/Inorganic Hybrid Proton Exchange Polymeric Membranes. *Chem. Mater.* **2006**, *18*, 69−75.
(24) Yang, H.-C.; Hou, J.; Chen, V.; Xu, Z.-K. Surface and Interface Engineering for Organic-Inorganic Composite Membranes. *J. Mater. Chem. A* **2016**, *4*, 9716−9729.
(25) Carbone, A.; Sacca, A.; Gatto, I.; Pedicini, R.; Passalacqua, E. Investigation on Composite S-Peek/H-Beta Meas for Medium Temperature Pefc. *Int. J. Hydrogen Energy* **2008**, *33*, 3153−3158.
(26) Di Vona, M. L.; Sgreccia, E.; Licoccia, S.; Khadhraoui, M.; Denoyel, R.; Knauth, P. Composite Proton-Conducting Hybrid Polymers: Water Sorption Isotherms and Mechanical Properties of Blends of Sulfonated Peek and Substituted PPSU. *Chem. Mater.* **2008**, *20*, 4327−4334.
(27) Donnadio, A.; Pica, M.; Carbone, A.; Gatto, I.; Posati, T.; Mariangeloni, G.; Casciola, M. Double Filler Reinforced Ionomers: A New Approach to the Design of Composite Membranes for Fuel Cell Applications. *J. Mater. Chem. A* **2015**, *3*, 23530−23538.
(28) Hasani-Sadrabadi, M. M.; Ghaffarian, S. R.; Mokarram-Dorri, N.; Dashtimoghadam, E.; Majedi, F. S. Characterization of Nanohybrid Membranes for Direct Methanol Fuel Cell Applications. *Solid State Ionics* **2009**, *180*, 1497−1504.
(29) He, Y.; Wang, J.; Zhang, H.; Zhang, T.; Zhang, B.; Cao, S.; Liu, J. Polydopamine-Modified Graphene Oxide Nanocomposite Membrane for Proton Exchange Membrane Fuel Cell under Anhydrous Conditions. *J. Mater. Chem. A* **2014**, *2*, 9548−9558.
(30) Heo, Y.; Im, H.; Kim, J. The Effect of Sulfonated Graphene Oxide on Sulfonated Poly (Ether Ether Ketone) Membrane for Direct Methanol Fuel Cells. *J. Membr. Sci.* **2013**, *425-426*, 11−22.
(31) Micali, N.; Villari, V.; Romeo, A.; Castriciano, M. A.; Scolaro, L. M. Evidence of the Early Stage of Porphyrin Aggregation by Enhanced Raman Scattering and Fluorescence Spectroscopy. *Phys. Rev. E* **2007**, *76*, 011404.
(32) Mossayebi, Z.; Sariri chi, T.; Rowshanzamir, S.; Parnian, M. J. Investigation and Optimization of Physicochemical Properties of Sulfated Zirconia/Sulfonated Poly (Ether Ether Ketone) Nanocomposite Membranes for Medium Temperature Proton Exchange Membrane Fuel Cells. *Int. J. Hydrogen Energy* **2016**, *41*, 12293−12306.
(33) Rangasamy, V. S.; Thayumanasundaram, S.; de Greef, N.; Seo, J. W.; Locquet, J.-P. Organic−Inorganic Hybrid Membranes Based on Sulfonated Poly(Ether Ether Ketone) and Tetrabutylphosphonium Bromide Ionic Liquid for Pem Fuel Cell Applications. *Eur. J. Inorg. Chem.* **2015**, *2015*, 1282−1289.
(34) Sambandam, S.; Ramani, V. Speek/Functionalized Silica Composite Membranes for Polymer Electrolyte Fuel Cells. *J. Power Sources* **2007**, *170*, 259−267.
(35) Campagne, B.; David, G.; Améduri, B.; Jones, D. J.; Rozière, J.; Roche, I. Novel Blend Membranes of Partially Fluorinated Copolymers Bearing Azole Functions with Sulfonated Peek for Pemfc Operating at Low Relative Humidity: Influence of the Nature of the N-Heterocycle. *Macromolecules* **2013**, *46*, 3046−3057.
(36) Li, H. T.; Zhang, G.; Ma, W. J.; Zhao, C. J.; Zhang, Y.; Han, M. M.; Zhu, J.; Liu, Z. G.; Wu, J.; Na, H. Composite Membranes Based on a Novel Benzimidazole Grafted Peek and Speek for Fuel Cells. *Int. J. Hydrogen Energy* **2010**, *35*, 11172−11179.
(37) Krishnan, N. N.; Henkensmeier, D.; Park, Y.-H.; Jang, J.-H.; Kwon, T.; Koo, C. M.; Kim, H.-J.; Han, J.; Nam, S.-W. Blue Membranes: Sulfonated Copper(Ii) Phthalocyanine Tetrasulfonic Acid Based Composite Membranes for Dmfc and Low Relative Humidity Pemfc. *J. Membr. Sci.* **2016**, *502*, 1−10.
(38) Kwon, T.; Cho, H.; Lee, J.-W.; Henkensmeier, D.; Kang, Y.; Koo, C. M. Sulfonated Copper Phthalocyanine/Sulfonated Polysulfone Composite Membrane for Ionic Polymer Actuators with High Power Density and Fast Response Time. *ACS Appl. Mater. Interfaces* **2017**, *9*, 29063−29070.
(39) Min, S.; Kim, D. Saxs Cluster Structure and Properties of Speek/Pei Composite Membranes for Dmfc Applications. *Solid State Ionics* **2010**, *180*, 1690−1693.
(40) Nagarale, R. K.; Gohil, G. S.; Shahi, V. K. Sulfonated Poly(Ether Ether Ketone)/Polyaniline Composite Proton-Exchange Membrane. *J. Membr. Sci.* **2006**, *280*, 389−396.
(41) Carbone, A.; Saccà, A.; Pedicini, R.; Gatto, I.; Passalacqua, E.; Romeo, A.; Scolaro, L. M.; Castriciano, M. A. Composite Speek-Tpyp Membranes Development for Portable Applications. *Int. J. Hydrogen Energy* **2015**, *40*, 17394−17401.
(42) Bruller, S.; Liang, H.-W.; Kramm, U. I.; Krumpfer, J. W.; Feng, X.; Mullen, K. Bimetallic Porous Porphyrin Polymer-Derived Non-Precious Metal Electrocatalysts for Oxygen Reduction Reactions. *J. Mater. Chem. A* **2015**, *3*, 23799−23808.
(43) Cantillo, N. M.; Goenaga, G. A.; Gao, W.; Williams, K.; Neal, C. A.; Ma, S.; More, K. L.; Zawodzinski, T. A. Investigation of a Microporous Iron(Iii) Porphyrin Framework Derived Cathode Catalyst in Pem Fuel Cells. *J. Mater. Chem. A* **2016**, *4*, 15621−15630.
(44) Li, J.; Song, Y.; Zhang, G.; Liu, H.; Wang, Y.; Sun, S.; Guo, X. Electrocatalysts: Pyrolysis of Self-Assembled Iron Porphyrin on Carbon Black as Core/Shell Structured Electrocatalysts for Highly Efficient Oxygen Reduction in Both Alkaline and Acidic Medium. *Adv. Funct. Mater.* **2017**, *27*, 1604356.
(45) Sonkar, P. K.; Prakash, K.; Yadav, M.; Ganesan, V.; Sankar, M.; Gupta, R.; Yadav, D. K. Co(Ii)-Porphyrin-Decorated Carbon Nanotubes as Catalysts for Oxygen Reduction Reactions: An Approach for Fuel Cell Improvement. *J. Mater. Chem. A* **2017**, *5*, 6263−6276.
(46) Chen, Z.; Lohr, A.; Saha-Möller, C. R.; Wurthner, F. Self-Assembled $\pi$-Stacks of Functional Dyes in Solution: Structural and Thermodynamic Features. *Chem. Soc. Rev.* **2009**, *38*, 564−584.
(47) Akins, D. L.; Zhu, H. R.; Guo, C. Absorption and Raman Scattering by Aggregated Meso-Tetrakis(P-Sulfonatophenyl)Porphine. *J. Phys. Chem.* **1994**, *98*, 3612−18.
(48) Castriciano, M. A.; Romeo, A.; De Luca, G.; Villari, V.; Scolaro, L. M.; Micali, N. Scaling the Chirality in Porphyrin J-Nanoaggregates. *J. Am. Chem. Soc.* **2011**, *133*, 765−767.
(49) Castriciano, M. A.; Romeo, A.; Zagami, R.; Micali, N.; Scolaro, L. M. Kinetic Effects of Tartaric Acid on the Growth of Chiral J-Aggregates of Tetrakis(4-Sulfonatophenyl)Porphyrin. *Chem. Commun.* **2012**, *48*, 4872−4874.
(50) Occhiuto, I. G.; Zagami, R.; Trapani, M.; Bolzonello, L.; Romeo, A.; Castriciano, M. A.; Collini, E.; Monsu Scolaro, L. The Role of Counter-Anions in the Kinetics and Chirality of Porphyrin J-Aggregates. *Chem. Commun.* **2016**, *52*, 11520−11523.
(51) Romeo, A.; Castriciano, M. A.; Occhiuto, I.; Zagami, R.; Pasternack, R. F.; Scolaro, L. M. Kinetic Control of Chirality in Porphyrin J-Aggregates. *J. Am. Chem. Soc.* **2014**, *136*, 40−43.
(52) Scolaro, L. M.; Romeo, A.; Castriciano, M. A.; Micali, N. Unusual Optical Properties of Porphyrin Fractal J-Aggregates. *Chem. Commun.* **2005**, 3018−3020.
(53) Zagami, R.; Romeo, A.; Castriciano, M. A.; Monsù Scolaro, L. Inverse Kinetic and Equilibrium Isotopic Effect on Self-Assembly and Supramolecular Chirality of Porphyrin J-Aggregates. *Chem. - Eur. J.* **2017**, *23*, 70−74.
(54) Castriciano, M. A.; Carbone, A.; Sacca, A.; Donato, M. G.; Micali, N.; Romeo, A.; De Luca, G.; Scolaro, L. M. Optical and Sensing Features of Tpps4 J-Aggregates Embedded in Nafion Membranes: Influence of Casting Solvents. *J. Mater. Chem.* **2010**, *20*, 2882−2886.
(55) Castriciano, M.; Romeo, A.; Villari, V.; Micali, N.; Scolaro, L. M. Nanosized Porphyrin J-Aggregates in Water/Aot/Decane Microemulsions. *J. Phys. Chem. B* **2004**, *108*, 9054−9059.


DOI: 10.1021/acsaem.8b00126
*ACS Appl. Energy Mater.* 2018, 1, 1664−1673

(56) Castriciano, M. A.; Romeo, A.; Villari, V.; Angelini, N.; Micali, N.; Scolaro, L. M. Aggregation Behavior of Tetrakis(4-Sulfonatophenyl)Porphyrin in Aot/Water/Decane Microemulsions. *J. Phys. Chem. B* **2005**, *109*, 12086−12092.
(57) Castriciano, M. A.; Romeo, A.; Villari, V.; Micali, N.; Scolaro, L. M. Structural Rearrangements in 5,10,15,20-Tetrakis(4-sulfonatophenyl)porphyrin J-Aggregates under Strongly Acidic Conditions. *J. Phys. Chem. B* **2003**, *107*, 8765−8771.
(58) Pasternack, R. F.; Collings, P. J. Resonance Light-Scattering - a New Technique for Studying Chromophore Aggregation. *Science* **1995**, *269*, 935−939.
(59) Kalyanasundaram, K. *Photochemistry of Polypyridine and Porphyrin Complexes*; Academic Press: London, 1992.
(60) Clarke, S. E.; Wamser, C. C.; Bell, H. E. *J. Phys. Chem. A* **2002**, *106*, 3235.
(61) Koti, A. S. R.; Taneja, J.; Periasamy, N. Control of Coherence Length and Aggregate Size in the J-Aggregate of Porphyrin. *Chem. Phys. Lett.* **2003**, *375*, 171−176.
(62) Castriciano, M. A.; Donato, M. G.; Villari, V.; Micali, N.; Romeo, A.; Scolaro, L. M. Surfactant-Like Behavior of Short-Chain Alcohols in Porphyrin Aggregation. *J. Phys. Chem. B* **2009**, *113*, 11173−11178.
(63) Maiti, N. C.; Ravikanth, M.; Mazumdar, S.; Periasamy, N. Fluorescence Dynamics of Noncovalently Linked Porphyrin Dimers, and Aggregates. *J. Phys. Chem.* **1995**, *99*, 17192−7.
(64) Ravikant, M.; Reddy, D.; Chandrashekar, T. K. Dimerization Effects on Spectroscopic Properties of Water-Soluble Porphyrins in Aqueous and Micellar Media. *J. Chem. Soc., Dalton Trans.* **1991**, 2103−2108.
(65) Luu, D. X.; Cho, E.-B.; Han, O. H.; Kim, D. Saxs and Nmr Analysis for the Cast Solvent Effect on Speek Membrane Properties. *J. Phys. Chem. B* **2009**, *113*, 12160−12160.
(66) Li, Y.; Peiffer, D. G.; Chu, B. Long-Range Inhomogeneities in Sulfonated Polystyrene Ionomers. *Macromolecules* **1993**, *26*, 4006−4012.
(67) Kreuer, K.-D.; Portale, G. A Critical Revision of the Nano-Morphology of Proton Conducting Ionomers and Polyelectrolytes for Fuel Cell Applications. *Adv. Funct. Mater.* **2013**, *23*, 5390−5397.
(68) Gandini, S. C. M.; Gelamo, E. L.; Itri, R.; Tabak, M. Small Angle X-Ray Scattering Study of Meso-Tetrakis (4-Sulfonatophenyl) Porphyrin in Aqueous Solution: A Self-Aggregation Model. *Biophys. J.* **2003**, *85*, 1259−1268.
(69) Schwab, A. D.; Smith, D. E.; Rich, C. S.; Young, E. R.; Smith, W. F.; de Paula, J. C. Porphyrin Nanorods. *J. Phys. Chem. B* **2003**, *107*, 11339−11345.
(70) El-Hachemi, Z.; Balaban, T. S.; Campos, J. L.; Cespedes, S.; Crusats, J.; Escudero, C.; Kamma-Lorger, C. S.; Llorens, J.; Malfois, M.; Mitchell, G. R.; Tojeira, A. P.; Ribó, J. M. Effect of Hydrodynamic Forces on Meso-(4-Sulfonatophenyl)-Substituted Porphyrin J-Aggregate Nanoparticles: Elasticity, Plasticity and Breaking. *Chem. - Eur. J.* **2016**, *22*, 9740−9749.
(71) El-Hachemi, Z.; Escudero, C.; Acosta-Reyes, F.; Casas, M. T.; Altoe, V.; Aloni, S.; Oncins, G.; Sorrenti, A.; Crusats, J.; Campos, J. L.; Ribo, J. M. Structure Vs. Properties - Chirality, Optics and Shapes - in Amphiphilic Porphyrin J-Aggregates. *J. Mater. Chem. C* **2013**, *1*, 3337−3346.
(72) Dong, C.; Wang, Q.; Cong, C.; Meng, X.; Zhou, Q. Influence of Alkaline 2d Carbon Nitride Nanosheets as Fillers for Anchoring Hpw and Improving Conductivity of Speek Nanocomposite Membranes. *Int. J. Hydrogen Energy* **2017**, *42*, 10317−10328.
(73) Gashoul, F.; Parnian, M. J.; Rowshanzamir, S. A New Study on Improving the Physicochemical and Electrochemical Properties of Speek Nanocomposite Membranes for Medium Temperature Proton Exchange Membrane Fuel Cells Using Different Loading of Zirconium Oxide Nanoparticles. *Int. J. Hydrogen Energy* **2017**, *42*, 590−602.
(74) Hasani-Sadrabadi, M. M.; Dashtimoghadam, E.; Sarikhani, K.; Majedi, F. S.; Khanbabaei, G. Electrochemical Investigation of Sulfonated Poly(Ether Ether Ketone)/Clay Nanocomposite Membranes for Moderate Temperature Fuel Cell Applications. *J. Power Sources* **2010**, *195*, 2450−2456.
(75) Jaafar, J.; Ismail, A. F.; Matsuura, T.; Nagai, K. Performance of Speek Based Polymer−Nanoclay Inorganic Membrane for Dmfc. *J. Membr. Sci.* **2011**, *382*, 202−211.
(76) Kim, A. R.; Vinothkannan, M.; Yoo, D. J. Sulfonated-Fluorinated Copolymer Blending Membranes Containing Speek for Use as the Electrolyte in Polymer Electrolyte Fuel Cells (Pefc). *Int. J. Hydrogen Energy* **2017**, *42*, 4349−4365.
(77) Li, D.; Guo, Q.; Zhai, W.; Tong, J.; Tan, X. Research on Properties of Speek Based Proton Exchange Membranes Doped with Ionic Liquids and Y2o3 in Different Humidity. *Procedia Eng.* **2012**, *36*, 34−40.
(78) Reinholdt, M. X.; Kaliaguine, S. Proton Exchange Membranes for Application in Fuel Cells: Grafted Silica/Speek Nanocomposite Elaboration and Characterization. *Langmuir* **2010**, *26*, 11184−11195.
(79) Salarizadeh, P.; Javanbakht, M.; Pourmahdian, S.; Beydaghi, H. Influence of Amine-Functionalized Iron Titanate as Filler for Improving Conductivity and Electrochemical Properties of Speek Nanocomposite Membranes. *Chem. Eng. J.* **2016**, *299*, 320−331.
(80) Sangeetha Rani, G.; Beera, M. K.; Pugazhenthi, G. Development of Sulfonated Poly(Ether Ether Ketone)/Zirconium Titanium Phosphate Composite Membranes for Direct Methanol Fuel Cell. *J. Appl. Polym. Sci.* **2012**, *124*, E45−E56.
(81) Wu, H.; Shen, X.; Cao, Y.; Li, Z.; Jiang, Z. Composite Proton Conductive Membranes Composed of Sulfonated Poly(Ether Ether Ketone) and Phosphotungstic Acid-Loaded Imidazole Microcapsules as Acid Reservoirs. *J. Membr. Sci.* **2014**, *451*, 74−84.
(82) Yen, Y.-C.; Ye, Y.-S.; Cheng, C.-C.; Lu, C.-H.; Tsai, L.-D.; Huang, J.-M.; Chang, F.-C. The Effect of Sulfonic Acid Groups within a Polyhedral Oligomeric Silsesquioxane Containing Cross-Linked Proton Exchange Membrane. *Polymer* **2010**, *51*, 84−91.
(83) Koziara, B. T.; Nijmeijer, K.; Benes, N. E. Optical Anisotropy, Molecular Orientations, and Internal Stresses in Thin Sulfonated Poly(Ether Ether Ketone) Films. *J. Mater. Sci.* **2015**, *50*, 3031−3040.
(84) Sgreccia, E.; Chailan, J. F.; Khadhraoui, M.; Di Vona, M. L.; Knauth, P. Mechanical Properties of Proton-Conducting Sulfonated Aromatic Polymer Membranes: Stress−Strain Tests and Dynamical Analysis. *J. Power Sources* **2010**, *195*, 7770−7775.
(85) Bras, W.; Dolbnya, I. P.; Detollenaere, D.; van Tol, R.; Malfois, M.; Greaves, G. N.; Ryan, A. J.; Heeley, E. Recent Experiments on a Small-Angle/Wide-Angle X-Ray Scattering Beam Line at the Esrf. *J. Appl. Crystallogr.* **2003**, *36*, 791−794.
(86) Micali, N.; Mallamace, F.; Castriciano, M.; Romeo, A.; Scolaro, L. M. Separation of Scattering and Absorption Contributions in Uv/Visible Spectra of Resonant Systems. *Anal. Chem.* **2001**, *73*, 4958−4963.
(87) Portale, G.; Cavallo, D.; Alfonso, G. C.; Hermida-Merino, D.; van Drongelen, M.; Balzano, L.; Peters, G. W. M.; Goossens, J. G. P.; Bras, W. Polymer Crystallization Studies under Processing-Relevant Conditions at the Saxs/Waxs Dubble Beamline at the Esrf. *J. Appl. Crystallogr.* **2013**, *46*, 1681−1689.
(88) Gatto, I.; Sacca, A.; Carbone, A.; Pedicini, R.; Urbani, F.; Passalacqua, E. Co-Tolerant Electrodes Developed with Phosphomolybdic Acid for Polymer Electrolyte Fuel Cell (Pefcs) Application. *J. Power Sources* **2007**, *171*, 540−545.


DOI: 10.1021/acsaem.8b00126
*ACS Appl. Energy Mater.* 2018, 1, 1664−1673